Spin-wave analysis of the spin-1 Heisenberg antiferromagnet with uniaxial single-ion anisotropy in a field

C. J. Hamer,[1] O. Rojas,[1,2] and J. Oitmaa[1]
[1]*School of Physics, The University of New South Wales, Sydney 2052, Australia*
[2]*Departamento de Ciencias Exatas, Universidade Federal de Lavras, CP 3037, 37200-000 Lavras, MG, Brazil*
(Received 9 March 2010; revised manuscript received 20 May 2010; published 17 June 2010)

Spin-wave approaches are explored for the spin-1 Heisenberg antiferromagnet with uniaxial single-ion anisotropy in a field. In the spin-flop region a standard $1/S$ expansion with canted quantization axes gives good results for small anisotropies or near the saturated ferromagnetic boundary. It is shown analytically that the formulation respects the Goldstone theorem through second order in $1/S$. For the square lattice case, we find that in the quantum paramagnetic phase a two-boson formulation gives good results at large anisotropies. Near the boundary of the quantum paramagnetic phase, neither approach gives good results and a more generalized approach is needed.

DOI: 10.1103/PhysRevB.81.214424 PACS number(s): 75.10.−b, 05.30.−d

I. INTRODUCTION

Following the claimed discovery of a remarkable "supersolid" behavior in solid ^{4}He,[1] a search has been proposed for analogous behavior in spin systems.[2–4] In fact using a Matsubara-Matsuda transformation,[5] one can transform directly from the relevant bosonic model to a lattice spin model. The spin-1/2 models are unrealistic, however, because they require the uniaxial exchange anisotropy to be too large.[3,6] Attention has therefore turned to spin-1 models and, in particular, the spin-1 Heisenberg antiferromagnet with uniaxial anisotropy in a magnetic field.

A number of magnetic materials have already been discovered which belong in this class. They include weakly coupled systems of linear chains such as $CsNiCl_3$,[7] with weak axial anisotropy, and more complex materials such as NENP $[Ni(C_2H_8N_2)_2HO_2(ClO_4)]$ (Ref. 8) and NENC $[Ni(C_2H_8N_2)_2Ni(CN_4)]$ (Ref. 9) with planar anisotropy. Recently Zvyagin *et al.*[10,11] have explored the excitation spectrum of DTN $[NiCl_2\text{-}4SC(NH_2)_2]$, another chain system with easy-plane anisotropy. None of these compounds appears to have the right parameters to give a supersolid phase however.

The Hamiltonian of the model is

$$\mathcal{H} = J\sum_{\langle i,j\rangle} (S_i^x S_j^x + S_i^y S_j^y + \Delta S_i^z S_j^z) + \sum_i (D(S_i^z)^2 - Sh_z S_i^z), \tag{1}$$

where $\langle i,j\rangle$ denotes nearest-neighbor pairs of sites, D is the single-ion anisotropy term, and Δ determines the uniaxial exchange anisotropy while h_z is the external magnetic field, rescaled by a factor S equal to the magnitude of the spin at each site. We shall set $J=1$ throughout this paper, unless it appears explicitly in the formulas.

The spin-1 version of the model has been discussed in a number of theoretical papers. Sengupta and Batista discussed the square lattice case[3] and the cubic lattice[4] using the stochastic series-expansion Monte Carlo method.[12] Holtschneider and co-workers[13–15] considered the classical model on a square lattice, using Monte Carlo techniques while Peters *et al.*[16] treated the linear-chain model using density-matrix renormalization-group methods. These authors found that a supersolid or "biconical" phase should exist over a range of magnetic fields for $D>0$ and $\Delta>1$. The model also exhibits other interesting phenomena such as magnetization plateaus[3,15,16] and a multicritical point.[15,16] Roscilde and Haas[17] used quantum Monte Carlo simulations to study the model.

Our aim here is to investigate spin-wave approaches to the problem. Spin-wave approaches to the simple Heisenberg antiferromagnet $(D=0,\Delta=1)$ in a field have been extensively discussed.[18–23] The zero-field case $(h_z=0,\Delta=1)$ has been treated by Papanicolaou and Spathis[24,25] and Oitmaa and Hamer,[26] who also carried out series-expansion studies of the model on a square lattice. Other numerical studies of the uniform case $(D=0)$ include finite-cell calculations by Yang and Mütter,[27] a high-order perturbation series calculation by Zheng Weihong *et al.*,[28] a coupled-cluster calculation by Wong *et al.*,[29] and exact diagonalization finite lattice calculations for the square lattice by Lin and Emery.[30] A Schwinger boson mean-field calculation for the zero-field case $(h_z=0)$ at large positive D has been carried out by Wang and Wang.[31]

In this preliminary investigation we treat the general case for arbitrary D and h_z but maintain $\Delta=1$, i.e., no exchange anisotropy. This restriction rules out the most interesting physical phenomena, unfortunately, such as a supersolid phase and multicritical points but still allows for some very interesting phase transitions. The restriction could be lifted quite easily but exploration of the supersolid region would require more elaborate and involved calculations.

The expected phase diagram for this case, derived from spin-wave and other theoretical approaches, is shown in Fig. 1 for the case of the square lattice. At large negative D and $h_z=0$, the model is in a standard antiferromagnetic (AF) Néel phase, with the spins aligned in the z direction ($S^z=\pm 1$ on alternating sites). At large positive D and $h_z=0$, there is a "quantum paramagnetic" (QPM) phase with $S^z=0$ at every site, so that all linear order parameters $\langle S^\alpha\rangle$ vanish and only a quadratic order parameter such as $Q_z=\langle \frac{2}{3}-(S_i^z)^2\rangle$ is nonzero. When h_z is very large, the system enters a saturated ferromagnetic (FM) phase, with all spins aligned in the z direction $(S_i^z=+1)$.

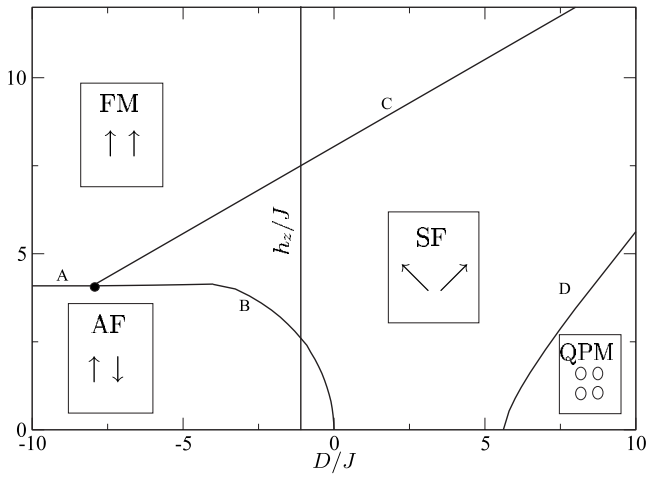

FIG. 1. Phase diagram for the square lattice, derived using spin-wave and series expansions.

Finally, in between these three regions is a fourth phase, the spin-flop (SF) phase with ferromagnetic order in the z direction M^z (provided $h_z \neq 0$) and antiferromagnetic order in the xy plane ($M_S^x \neq 0$, say), which spontaneously breaks the planar $U(1)$ symmetry of the model. The Goldstone theorem then requires that the system should exhibit a gapless Goldstone mode in this region. One of the issues to be explored in this paper is whether a spin-wave treatment conforms with the Goldstone theorem. The transitions between the AF phase and FM or SF phase are expected to be first order while the transition between the QPM and SF phases, and the SF and FM phases, are expected to be second order.

The layout of the paper is as follows. In Sec. II, we shall present a spin-wave treatment of the SF phase and show that the Goldstone theorem is obeyed through second order in a $1/S$ expansion. In Sec. III we shall discuss a spin-wave treatment of the QPM phase and in Sec. IV the AF phase is treated very briefly. Finally, in Sec. V our conclusions are summarized.

II. SPIN-FLOP PHASE AT NONZERO h_z

In the SF phase according to classical theory, the spins will be ordered in a canted fashion as shown in Fig. 1, with ferromagnetic order in the z direction and antiferromagnetic order in the xy plane. We assume a bipartite lattice, and choose quantization axes on the two sublattices A and B as shown in Fig. 2, assuming that at zeroth order the spins are in the xz plane, at a canting angle θ to the x axis. With respect to the new quantization axes (z', x'), the Hamiltonian now takes the form

$$\mathcal{H} = J\sum_{\langle i,j\rangle}[S_i^y S_j^y - (S_i^x S_j^x + S_i^z S_j^z)\cos 2\theta + \eta_i(S_i^z S_j^x - S_i^x S_j^z)\sin 2\theta]$$
$$+ D\sum_i \left[(S_i^z)^2 \sin^2\theta + (S_i^x)^2\cos^2\theta + \frac{\eta_i}{2}(S_i^z S_i^x + S_i^x S_i^z)\sin 2\theta\right] - Sh_z\sum_i (S_i^z \sin\theta + \eta_i S_i^x \cos\theta), \quad (2)$$

where

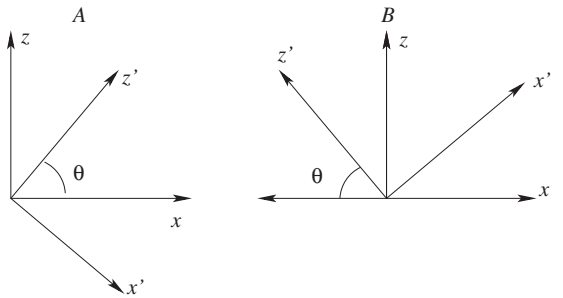

FIG. 2. The quantization axes for two sublattices A and B, assuming that at zeroth order the spins are in the xz plane, at a canting angle θ to the x axis.

$$\eta_i = \begin{cases} +1, & i \in B \\ -1, & i \in A. \end{cases} \quad (3)$$

First, we follow the standard spin-wave procedure and introduce boson creation and annihilation operators $a_i^\dagger$ and a_i by means of a standard Holstein-Primakoff transformation[32] so that at each site i we replace

$$S_i^z = S - a_i^\dagger a_i,$$

$$S_i^+ = \sqrt{2S}\left(1 - \frac{a_i^\dagger a_i}{4S}\right)a_i + \cdots,$$

$$S_i^- = \sqrt{2S}a_i^\dagger\left(1 - \frac{a_i^\dagger a_i}{4S}\right) + \cdots, \quad (4)$$

keeping only the leading terms in a $1/S$ expansion. Through second order in S, this results in a bosonic Hamiltonian, given in Appendix A by Eq. (A1).

Next, we perform a Fourier transformation

$$a_{\mathbf{k}} = \sqrt{\frac{1}{N}}\sum_m e^{i\mathbf{k}\cdot R_m} a_m, \quad (5)$$

leading to the momentum space version of Hamiltonian (A1) given in Appendix A by Eq. (A2).

Finally, we aim to diagonalize the Hamiltonian through quadratic terms by means of a Bogoliubov transformation

$$a_{\mathbf{k}} = u_{\mathbf{k}}\alpha_{\mathbf{k}} + v_{\mathbf{k}}\alpha_{-\mathbf{k}}^\dagger, \quad (6)$$

where $u_{\mathbf{k}} = \cosh\Theta_{\mathbf{k}}$, $v_{\mathbf{k}} = \sinh\Theta_{\mathbf{k}}$, and $\Theta_{\mathbf{k}} = \Theta_{-\mathbf{k}}$.

Terms in the Hamiltonian must now be normal ordered with respect to the $\{\alpha_k\}$ vacuum using Wick's Theorem, which requires some algebra. It is then convenient to express the results first in terms of combinations of the old operators $a_k^\dagger$ and a_k,

$$\mathcal{H} = N\mathcal{E}_0 + \sqrt{N}\mathcal{C}:a_{\mathbf{Q}} + a_{\mathbf{Q}}^\dagger: + \sum_{\mathbf{k}}\left[\mathcal{A}_{\mathbf{k}}:a_{\mathbf{k}}^\dagger a_{\mathbf{k}}: + \frac{\mathcal{B}_{\mathbf{k}}}{2}:a_{\mathbf{k}}^\dagger a_{-\mathbf{k}}^\dagger + a_{\mathbf{k}}a_{-\mathbf{k}}:\right] + \frac{1}{\sqrt{N}}\sum_{1,2,3}\delta_{\mathbf{1+2-3-Q}}\mathcal{D}^{(1)}[:a_1^\dagger a_2^\dagger a_3 + a_3^\dagger a_2 a_1:]$$
$$+ \frac{1}{\sqrt{N}}\sum_{1,2,3}\delta_{\mathbf{1-2-3-Q}}\mathcal{D}^{(2)}[:a_1^\dagger a_2 a_3 + a_3^\dagger a_2^\dagger a_1:]\gamma_3 + \text{quartic terms}, \quad (7)$$

where the colons indicate normal ordered products with respect to the new $\{\alpha_k\}$ vacuum and $\mathbf{Q}$ is the Néel momentum [(π,π) for the square lattice]. The coefficient functions appearing here are listed in Appendix A.

The linear term in $[:a_{\mathbf{Q}}+a_{\mathbf{Q}}^{\dagger}:]$ indicates an instability, so we must require that this term vanish, $\mathcal{C}=0$, which implies either $\cos\theta=0$, i.e., $\theta=\pi/2$, corresponding to complete ferromagnetic order in the z direction; or else,

$$\sin\theta=\frac{h_z}{2}\left[1-\frac{(2T_1+T_2)}{4S}\right]\left[(zJ+D)-\frac{(2T_1+T_2)(5D+zJ)}{4S}-\frac{D}{2S}+\frac{zJ(-T_1+T_3+T_4)}{S}\right]^{-1}, \tag{8}$$

where the quantities T_i, $i=\{1,\ldots,4\}$ are contraction sums defined in Appendix A which arise from quantum fluctuations.

This condition determines the canting angle θ. At leading order in $1/S$, it simply gives the classical result. At next order, quantum corrections due to T_1, T_2, T_3, and T_4 come in.

To diagonalize the quadratic terms using the Bogoliubov transformation (6) we require

$$\tanh 2\Theta_{\mathbf{k}}=\frac{2u_{\mathbf{k}}v_{\mathbf{k}}}{u_{\mathbf{k}}^2+v_{\mathbf{k}}^2}=-\frac{\mathcal{B}_{\mathbf{k}}}{\mathcal{A}_{\mathbf{k}}} \tag{9}$$

and the contraction terms can now be expressed in terms of the functions $\mathcal{A}_{\mathbf{k}}$ and $\mathcal{B}_{\mathbf{k}}$ (defined in Appendix A) as

$$T_1=\frac{1}{2N}\sum_{\mathbf{k}}\left(\frac{\mathcal{A}_{\mathbf{k}}}{\omega_{\mathbf{k}}}-1\right),$$

$$T_2=\frac{-1}{2N}\sum_{\mathbf{k}}\frac{\mathcal{B}_{\mathbf{k}}}{\omega_{\mathbf{k}}},$$

$$T_3=\frac{1}{2N}\sum_{\mathbf{k}}\frac{\mathcal{A}_{\mathbf{k}}\gamma_{\mathbf{k}}}{\omega_{\mathbf{k}}},$$

$$T_4=\frac{-1}{2N}\sum_{\mathbf{k}}\frac{\mathcal{B}_{\mathbf{k}}\gamma_{\mathbf{k}}}{\omega_{\mathbf{k}}}, \tag{10}$$

where

$$\omega_{\mathbf{k}}=\sqrt{\mathcal{A}_{\mathbf{k}}^2-\mathcal{B}_{\mathbf{k}}^2}. \tag{11}$$

The Hamiltonian now takes the final form

$$\mathcal{H}=N\mathcal{E}_0+\sum_{\mathbf{k}}\omega_{\mathbf{k}}\alpha_{\mathbf{k}}^{\dagger}\alpha_{\mathbf{k}}+\sqrt{\frac{S}{2N}}\sum_{1-3}\delta_{\mathbf{1+2+3-Q}}(\alpha_1^{\dagger}\alpha_2^{\dagger}\alpha_3^{\dagger}+\text{H.c.})\Phi^{(1)}(1,2,3)+\sqrt{\frac{S}{2N}}\sum_{1-3}\delta_{\mathbf{1+2-3-Q}}(\alpha_1^{\dagger}\alpha_2^{\dagger}\alpha_3+\text{H.c.})\Phi^{(2)}(1,2,3)+\text{quartic terms}, \tag{12}$$

where $\mathcal{E}_0$ is given by Eq. (A3) and the symmetrized forms of the three-particle vertex functions are

$$\Phi^{(1)}(1,2,3)=\frac{1}{12}[h_z\cos\theta-(5D+zJ)\sin 2\theta](u_1u_2v_3+u_1v_2v_3+u_1v_2u_3+v_1v_2u_3+u_1v_2u_3+v_1u_2v_3)+\frac{zJ}{6}\sin 2\theta[\gamma_3(u_3+v_3)(u_1v_2+v_1u_2)+\gamma_1(u_1+v_1)(u_2v_3+v_2u_3)+\gamma_2(u_2+v_2)(u_1v_3+v_1u_3)], \tag{13}$$

$$\Phi^{(2)}(1,2,3)=\frac{1}{4}[h_z\cos\theta-(5D+zJ)\sin 2\theta][u_1u_2u_3+(u_1v_2+v_1u_2)(u_3+v_3)+v_1v_2v_3]+\frac{zJ}{2}\sin 2\theta[\gamma_3(u_3+v_3)(u_1v_2+v_1u_2)+\gamma_1(u_1+v_1)(u_2u_3+v_2v_3)+\gamma_2(u_2+v_2)(u_1u_3+v_1v_3)]. \tag{14}$$

The three-particle interaction terms have been discussed by Osano *et al.*[18] and Zhitomirsky and Chernyshev.[22] They imply that at strong magnetic fields h_z the one magnon state becomes unstable to spontaneous two-magnon decay.

A. Order parameters

The ferromagnetic order in the (original) z direction is given by

$$M^z=\frac{1}{N}\left\langle\sum_i S_i^z\right\rangle_0=\frac{1}{N}\sum_i\langle[S_i^z\sin\theta+\eta_iS_i^x\cos\theta]\rangle_0 \tag{15}$$

in terms of the new axes of Fig. 2. Through second order in $1/S$, this reduces to

$$M^z=\frac{1}{N}\sum_i\langle(S-a_i^{\dagger}a_i)\sin\theta\rangle_0=(S-T_1)\sin\theta. \tag{16}$$

Similarly, the staggered magnetization in the x direction is given by

$$M_S^x=\frac{1}{N}\sum_i\langle\eta_iS_i^x\rangle_0=\frac{1}{N}\sum_i\langle(S-a_i^{\dagger}a_i)\cos\theta\rangle_0=(S-T_1)\cos\theta. \tag{17}$$

B. One-particle excitation spectrum and Goldstone theorem

At leading order in the $1/S$ expansion,

$$\mathcal{A}_{\mathbf{k}}=S[zJ(\cos 2\theta+\gamma_{\mathbf{k}}\sin^2\theta)+D(1-3\sin^2\theta)+h_z\sin\theta], \tag{18}$$

$$\mathcal{B}_{\mathbf{k}}=S(D-zJ\gamma_{\mathbf{k}})\cos^2\theta, \tag{19}$$

Using Eq. (8) $\mathcal{A}_{\mathbf{k}}$ can be rewritten at leading order,

$$\mathcal{A}_{\mathbf{k}}=SzJ(1+\gamma_{\mathbf{k}})+S(D-zJ\gamma_{\mathbf{k}})\cos^2\theta. \tag{20}$$

Hence it is easily seen that as $\mathbf{k}\to\mathbf{Q}$ and $\gamma_{\mathbf{k}}\to-1$, then $\mathcal{A}_{\mathbf{k}}-\mathcal{B}_{\mathbf{k}}\to 0$ and $\omega_{\mathbf{k}}\to 0$ so that the Goldstone theorem is

satisfied, and the one-particle excitation energy vanishes at the Néel momentum **Q**, corresponding to spontaneous breakdown of the original $U(1)$ symmetry.

Does the same result hold at higher orders in the $1/S$ expansion? The $U(1)$ symmetry of the original Hamiltonian is hidden in the spin-wave version [Eq. (7)] but nevertheless, if the theorem is respected at leading order in the $1/S$ expansion, one would expect it also to be respected at higher orders. Zhitomirski and Nikuni[20] showed numerical evidence that it was respected at second order for the case $D=0$. Here we show analytically that the theorem holds to second order in the general case. Since the proof is rather long, we relegate it to Appendix B.

C. Singular behavior near $h_{z,cC}$

It was shown by Zhitomirsky and Nikuni[20] that at $D=0$ the contraction sum T_1, and hence the magnetization, displays a logarithmic singularity as $h_z \to h_{z,cC}$, the phase boundary with the FM phase. Similarly in the general case, if we calculate T_1 in leading order, then near the phase boundary we find

$$T_1 \sim \frac{(zJ+D)p}{\pi zJ} \ln\left[\frac{\pi^2 zJ}{4(zJ+D)p}\right], \quad p \to 0, \tag{21}$$

where $p=(h_{z,cC}-h_z)/h_{z,cC}$.

D. Numerical results

We have computed values for the physical parameters as function of D and h_z to first and second orders in a $1/S$ expansion, setting $S=1$ and $z=4$ as appropriate for the square lattice. First we consider the case $D=0$, considered previously by Zhitomirsky and Nikuni[20,21] for the case $S=1/2$. Figure 3(a) shows the canting angle θ as a function of h_z while Fig. 3(b) gives the ferromagnetic component of the magnetization M^z and Fig. 3(c) the staggered component M_s^x. Finally, Fig. 3(d) shows the transverse susceptibility

$$\chi_T = \frac{\partial M_s^x}{\partial h_z}. \tag{22}$$

It can be seen that there is very little difference between the first- and second-order results in this case, indicating that the spin-wave results are quite accurate for $D=0$. As a calibration point, the spin-wave estimate for M_s^x at $D=0$ and $h_z=0$ is 0.8034, to be compared with estimates 0.8039(4) from high-order perturbation series[28] and 0.767(4) from a finite-lattice calculation.[30] There is also little sign in the magnetization M^z of the logarithmic singularity implied by Eq. (21); it is more obvious for the case $S=1/2$.[20] We find that M^z increases monotonically to its saturation value at $h_{z,cC}$. The staggered magnetization M_s^x, by contrast, first increases slightly as the quantum fluctuations decrease and then drops away to zero at $h_{z,cC}$. This behavior was previously noticed by Zhitomirsky and Nikuni for the case $S=1/2$.[20]

Figure 4 gives some similar results at a finite value of the axial anisotropy $D=1$. Figure 4(a) shows the canting angle θ, and Figs. 4(b) and 4(c) the magnetizations M^z and M_s^x, as functions of h_z. The open squares in Figs. 4(b) and 4(c) are series estimates at small h_z, which agree well with the spin-wave results. This time, a substantial difference can be seen between first- and second-order results, illustrating the need to go to second order. Otherwise, the qualitative behavior is similar to that at $D=0$.

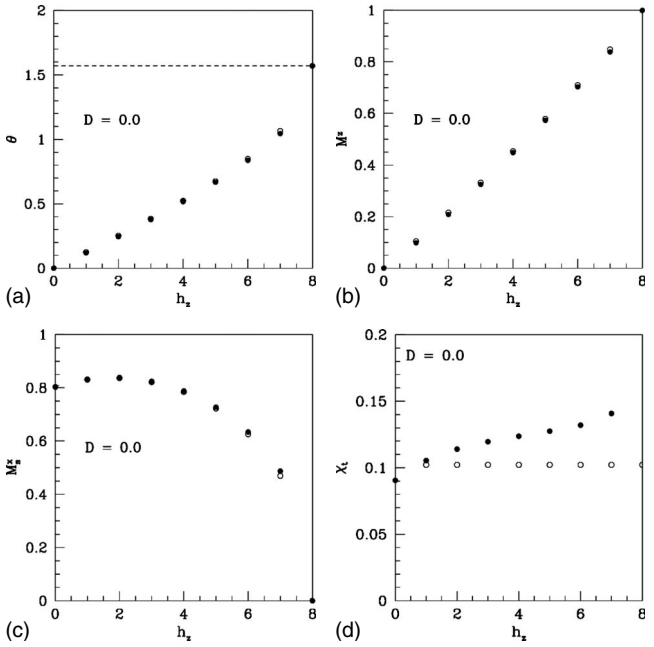

FIG. 3. Spin-wave calculations for the square lattice of (a) canting angle θ; (b) magnetization M^z; (c) staggered magnetization M_S^x; and (d) transverse (staggered) susceptibility χ_t in the SF phase as functions of h_z, for the case $D=0$. Open circles: first-order results and filled circles: second-order results.

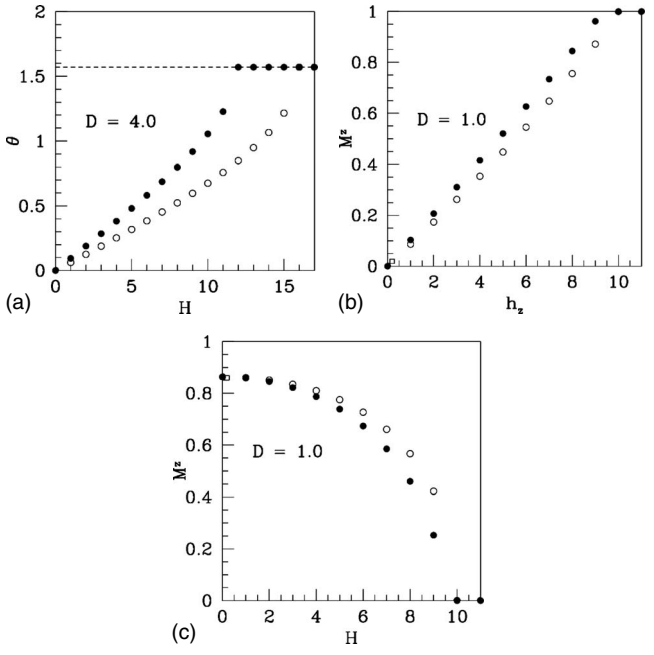

FIG. 4. Spin-wave calculations for the square lattice of (a) canting angle θ; (b) magnetization M^z; and (c) staggered magnetization M_s^x as functions of h_z, for the case $D=1$. Conventions as in Fig. 3.

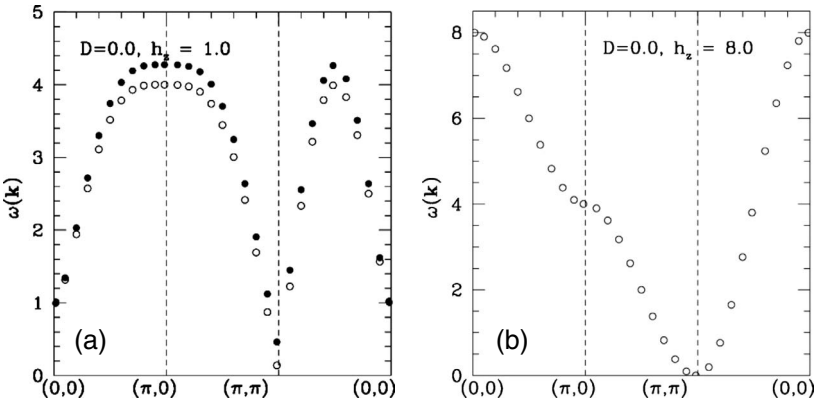

FIG. 5. Spin-wave dispersion relations for the square lattice at (a) $D=0$ and $h_z=1$; and (b) $D=0$ and $h_z=8$. Conventions as for Fig. 3.

Figure 5(a) shows the single-particle dispersion relation at $D=0$ and $h_z=1$ and Fig. 5(b) the relation at $D=0$ and $h_z=8$. It can be seen that at finite h_z a finite-energy gap opens up at $\mathbf{k}=0$ and becomes larger with h_z. The gap at $\mathbf{Q}=(\pi,\pi)$ remains zero at all h_z, however, in accordance with the Goldstone theorem. (Note that the point graphed nearest to (π,π) is at a slightly lower momentum. The first-order result explicitly vanishes at (π,π); the second-order calculations become singular in that neighborhood, as shown in Appendix B, so the calculated number is a little high).

Figure 6 shows the spin-wave velocity c as a function of h_z at $D=0$. It can be seen that the spin-wave velocity (the slope of the dispersion relation at $\mathbf{k}=\mathbf{Q}$) goes to zero as $h_z \to h_{z,cC}$, and correspondingly the dispersion relation becomes quadratic in that neighborhood, as seen in Fig. 5(b).

If we assume that the hydrodynamic relation[33] holds

$$\frac{\chi_T c^2}{\rho_S} = 1, \tag{23}$$

then the spin stiffness ρ_S will vanish along with the spin-wave velocity c as $h_z \to h_{z,cC}$. This argument has recently been verified by Chernyshev and Zhitomirsky[23] for the case $S=1/2$ and $D=0$.

Finally, Fig. 7 shows the staggered magnetization M_s^x as a function of D for zero magnetizatic field h_z, together with earlier series expansion estimates from Oitmaa and Hamer.[26] It can be seen that the series and spin-wave estimates agree quite well at small D but the spin-wave results fail to reproduce the plunge in the magnetization toward the critical point at $D \simeq 5.6$ marking the transition to the QPM phase.

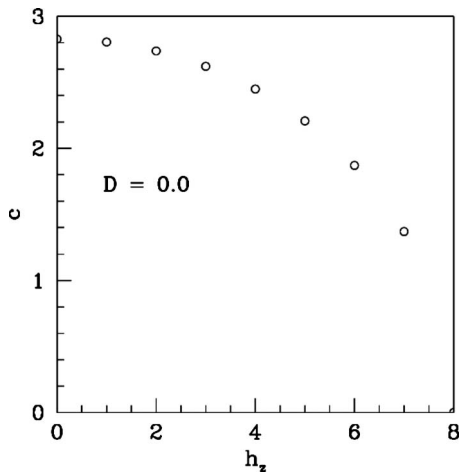

FIG. 6. Spin-wave velocity c for the square lattice as a function of h_z at $D=0$. First-order spin-wave results only.

III. QUANTUM PARAMAGNETIC PHASE

Here we adopt a formalism specific to $S=1$. As $D \to \infty$, the ground state is $|0\rangle = |\{S_i^z = 0, \text{ all } i\}\rangle$, so we take this as our vacuum state. We then introduce bosonic creation and annihilation operators $b_{i,\pm}^\dagger$ and $b_{i,\pm}$, at each site i (for states $S^z = \pm 1$, respectively), obeying $b_{i,\pm}|0\rangle = 0$. The corresponding Holstein-Primakoff transformation is

$$\begin{aligned} S_i^z &= n_{i,+} - n_{i,-}, \\ S_i^+ &= \sqrt{2}[b_{i,+}^\dagger P_i + P_i b_{i,-}], \\ S_i^- &= \sqrt{2}[b_{i,-}^\dagger P_i + P_i b_{i,+}], \end{aligned} \tag{24}$$

where $n_{i,\pm} = b_{i,\pm}^\dagger b_{i,\pm}$ and $P_i = \sqrt{1 - n_{i,+} - n_{i,-}}$. This transformation satisfies the correct spin algebra in the physical subspace and forbids transitions from inside to outside it. Expanding

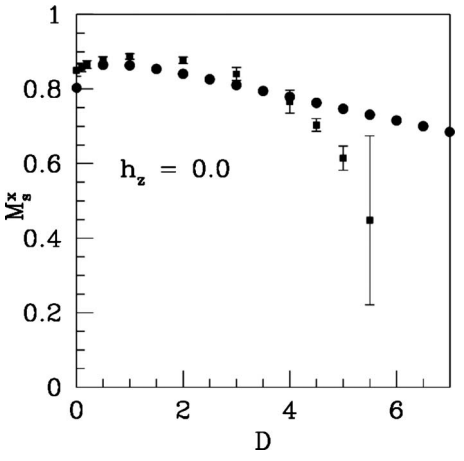

FIG. 7. Staggered magnetization M_S^x for the square lattice in the SF phase as a function of D at $h_z=0$. Points with error bars are series estimates (Ref. 26) and filled circles are spin-wave results.

the square root to first order in $n_{i,+}+n_{i,-}$, we find

$$\mathcal{H} = D\sum_i (n_{i,+}+n_{i,-}) - h_z\sum_i (n_{i,+}-n_{i,-}) + J\sum_{\langle i,j\rangle}\Bigg\{(n_{i,+}-n_{i,-}) \times (n_{j,+}-n_{j,-}) + [(b^\dagger_{i,+}+b_{i,-})(b^\dagger_{j,+}+b_{j,-})+\text{H.c.}] - \frac{1}{2}\sum_{\sigma=\pm}\{[b^\dagger_{i,\sigma}(n_{i,+}+n_{i,-})+(n_{i,+}+n_{i,-})b_{i,-\sigma}] \times (b^\dagger_{j,-\sigma}+b_{j,\sigma})+\text{H.c.}\}\Bigg\}, \tag{25}$$

where we have "linearized" $(S_i^z)^2 = n_{i,+}n_{i,-}$, as appropriate to the physical subspace.

Next, use Fourier transformation

$$b_{\mathbf{k},\pm} = \sqrt{\frac{1}{N}}\sum_n e^{i\mathbf{k}\cdot\mathbf{R}_n} b_{n,\pm} \tag{26}$$

to obtain

$$\mathcal{H} = \sum_{\mathbf{k}}\Bigg[\sum_{\sigma=\pm}(D+zJ-\sigma h_z)b^\dagger_{\mathbf{k},\sigma}b_{\mathbf{k},\sigma} + zJ\gamma_{\mathbf{k}}(b^\dagger_{\mathbf{k},+}b^\dagger_{-\mathbf{k},-} + \text{H.c.})\Bigg] + \frac{zJ}{4N}\sum_{1,2,3,4}\{\delta_{1+2-3-4}\Bigg[\sum_{\sigma=\pm} b^\dagger_{1,\sigma}b^\dagger_{2,\sigma}b_{3,\sigma}b_{4,\sigma}(2\gamma_{2-4} - \gamma_4-\gamma_1-\gamma_3-\gamma_2) - 2b^\dagger_{1,+}b^\dagger_{2,-}b_{3,+}b_{4,-} \times(\gamma_{2-4}+\gamma_{1-3}+\gamma_4+\gamma_1+\gamma_3+\gamma_2)\Bigg] - \delta_{1+2+3-4} \times [(b^\dagger_{1,+}b^\dagger_{2,+}b^\dagger_{3,-}b_{4,+}+\text{H.c.})(2\gamma_3+\gamma_2+\gamma_1) + (b^\dagger_{1,+}b^\dagger_{2,-}b^\dagger_{3,-}b_{4,-}+\text{H.c.})(2\gamma_1+\gamma_2+\gamma_3)]\} + (\text{six-body terms}). \tag{27}$$

Then perform a Bogoliubov transformation

$$\beta_{\mathbf{k},\pm} = u_{\mathbf{k}}b_{\mathbf{k},\pm} + v_{\mathbf{k}}b^\dagger_{-\mathbf{k},\mp} \tag{28}$$

to obtain

$$\mathcal{H} = N\mathcal{E}_0 + \sum_{\mathbf{k}}(\beta^\dagger_{\mathbf{k},+}\beta_{\mathbf{k},+}+\beta^\dagger_{\mathbf{k},-}\beta_{\mathbf{k},-})[(u_{\mathbf{k}}^2+v_{\mathbf{k}}^2)\mathcal{A}_{\mathbf{k}} + 2u_{\mathbf{k}}v_{\mathbf{k}}\mathcal{B}_{\mathbf{k}}] - \sum_{\mathbf{k}}(\beta^\dagger_{\mathbf{k},+}\beta^\dagger_{-\mathbf{k},-}+\beta_{\mathbf{k},+}\beta_{-\mathbf{k},-})[(u_{\mathbf{k}}^2+v_{\mathbf{k}}^2)\mathcal{B}_{\mathbf{k}} + 2u_{\mathbf{k}}v_{\mathbf{k}}\mathcal{A}_{\mathbf{k}}] + h_z\sum_{\mathbf{k}}(\beta^\dagger_{\mathbf{k},-}\beta_{\mathbf{k},-}-\beta^\dagger_{\mathbf{k},+}\beta_{\mathbf{k},+}), \tag{29}$$

where

$$\mathcal{E}_0 = 2[DT_1 + zJ(T_3-T_4)] + zJ[T_3^2 - T_4^2 + 2(T_4-T_3)(3T_1 - T_2)], \tag{30}$$

$$\mathcal{A}_{\mathbf{k}} = D + zJ[\gamma_{\mathbf{k}} + 3(T_4-T_3) + \gamma_{\mathbf{k}}(T_3+T_2-3T_1)], \tag{31}$$

$$\mathcal{B}_{\mathbf{k}} = -zJ[\gamma_{\mathbf{k}} - T_4 - T_3 - \gamma_{\mathbf{k}}(T_4+T_2+3T_1)] \tag{32}$$

(using a notation conforming with the previous section) and the contraction sums $T_1,\ldots,T_4$ are defined in Eq. (A9).

To diagonalize the quadratic terms in $\mathcal{H}$, we require

$$\tan 2\Theta_{\mathbf{k}} = \frac{2u_{\mathbf{k}}v_{\mathbf{k}}}{u_{\mathbf{k}}^2+v_{\mathbf{k}}^2} = -\frac{\mathcal{B}_{\mathbf{k}}}{\mathcal{A}_{\mathbf{k}}}, \tag{33}$$

whence through second-order terms

$$\mathcal{H} = N\mathcal{E}_0 + \sum_{\mathbf{k}}[\omega_{\mathbf{k}}(\beta^\dagger_{\mathbf{k},+}\beta_{\mathbf{k},+}+\beta^\dagger_{\mathbf{k},-}\beta_{\mathbf{k},-}) + h_z(\beta^\dagger_{\mathbf{k},-}\beta_{\mathbf{k},-}-\beta^\dagger_{\mathbf{k},+}\beta_{\mathbf{k},+})], \tag{34}$$

where

$$\omega_{\mathbf{k},\pm} = \sqrt{\mathcal{A}_{\mathbf{k}}^2-\mathcal{B}_{\mathbf{k}}^2} \mp h_z \tag{35}$$

and the contraction sums $T_1,\ldots,T_4$ are once again given by Eq. (10).

Note that h_z plays a trivial role in this phase, producing a simple Zeeman energy shift proportional to S_i^z. The single-particle excitation energy $\omega_{\mathbf{k}}$ at $h_z=0$ is gapped, with the minimum gap occurring at $\mathbf{k}=\mathbf{Q}$ and $\gamma_{\mathbf{k}}=-1$. At leading order, we find $\omega_{\mathbf{Q}}=\sqrt{D^2-2zJD}$. At finite h_z the one-particle excitation energy with $S^z=+1$ is

$$\epsilon_{\mathbf{Q}}^{+1} = \omega_{\mathbf{Q}} - h_z. \tag{36}$$

This vanishes at

$$h_{z,cD} = \omega_{\mathbf{Q}} = \sqrt{D(D-2zJ)}, \tag{37}$$

marking the boundary of the QPM phase. Note that the energies of all other excited states with positive total S^z vanish at the same point, indicating that the transition is second order. Note also that the ground state still has $S^z=0$ at all h_z values until the transition point $h_{z,cD}$ is reached. At $h_z=0$, the critical point lies at $D=2zJ$, in leading order. At second order, a numerical calculation is required to calculate $\omega_{\mathbf{k}}$.

A. Order parameters

The linear order parameters $\langle S_i^\alpha\rangle_0$ are all zero in this "paramagnetic" phase.

A convenient second-order parameter is

$$Q_z = \frac{2}{3} - \langle (S_i^z)^2\rangle = \frac{2}{3} - \frac{1}{N}\sum_i \langle n_{i,+}+n_{i,-}\rangle = 2\left(\frac{1}{3}-T_1\right). \tag{38}$$

B. Numerical results

We have calculated physical quantities as functions of D for zero magnetic field h_z, both for the first-order theory, and the self-consistent second-order theory, for the square lattice. Figure 8 shows the ground-state energy per site as a function of D. It can be seen that the spin-wave results are accurate enough at large D but deviate from the series estimates at smaller D, indicating the need for higher-order corrections.

Figure 9 shows the energy gap at $Q=(\pi,\pi)$ as a function of D, along with perturbation series results from Oitmaa and Hamer.[26] It can be seen that the second-order spin-wave estimates agree well with the series estimates at large D, but run too high at smaller D, while the first-order results are too low, as compared with the estimate $D_c \simeq 5.47$ of Wang and

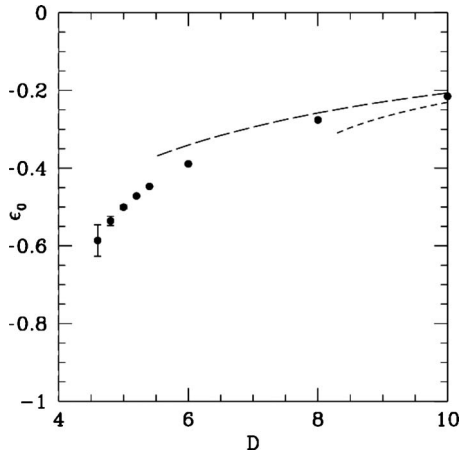

FIG. 8. Ground-state energy per site for the square lattice in the QPM phase as a function of D at $h_z=0$. Points with error bars are series estimates (Ref. 26); short-dashed line: first-order spin-wave; and long-dashed line: second-order spin-wave results.

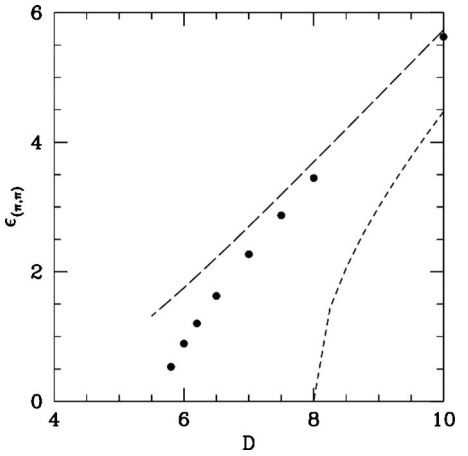

FIG. 9. Energy gap for the square lattice in the QPM phase as a function of D at $h_z=0$. Conventions as in Fig. 8.

Wang,[31] or the series estimates which indicate $D_c \simeq 5.6$, consistent with the Monte Carlo result $D_c=5.65(2)$ obtained by Roscilde and Haas.[17]

Figure 10 shows the quadratic order parameter Q_Z as a function of D. Neither spin-wave nor series estimates show any clear sign of the QPM phase boundary here. As usual, the order parameter would be expected to dive sharply very near the boundary.

IV. NÉEL PHASE

A spin-wave theory for this phase in the case $h_z=0$ was briefly considered by Oitmaa and Hamer,[26] and the effect of the magnetic field h_z is again rather trivial in this case. We shall use their formulation here. The initial Hamiltonian $\mathcal{H}$, Eq. (1), is expressed in terms of boson operators a_i and b_j on sublattices A and B via a Dyson-Maleev transformation,

$$A:\begin{cases} S_i^z &= S - a_i^\dagger a_i, \\ S_i^+ &= \sqrt{2S}(1 - a_i^\dagger a_i/2S)a_i, \\ S_i^- &= \sqrt{2S}a_i^\dagger, \end{cases} \tag{39}$$

$$B:\begin{cases} S_j^z &= b_j^\dagger b_j - S, \\ S_j^+ &= \sqrt{2S}b_j^\dagger(1 - b_j^\dagger b_j/2S), \\ S_j^- &= \sqrt{2S}b_j, \end{cases} \tag{40}$$

followed by a Fourier transformation

$$a_i = \sqrt{\frac{2}{N}}\sum_{\mathbf{k}} e^{-i\mathbf{k}\cdot\mathbf{R}_i}a_{\mathbf{k}}, \quad b_j = \sqrt{\frac{2}{N}}\sum_{\mathbf{k}} e^{-i\mathbf{k}\cdot\mathbf{R}_j}b_{\mathbf{k}}, \tag{41}$$

giving

$$\begin{aligned}\mathcal{H} = &-\frac{1}{2}NS^2(zJ-2D) + zJS\sum_{\mathbf{k}}(a_{\mathbf{k}}^\dagger b_{\mathbf{k}}^\dagger + a_{\mathbf{k}}b_{\mathbf{k}})\gamma_{\mathbf{k}} \\ &+ [S(zJ-2D)+D]\sum_{\mathbf{k}}(a_{\mathbf{k}}^\dagger a_{\mathbf{k}} + b_{\mathbf{k}}^\dagger b_{\mathbf{k}}) \\ &- \frac{zJ}{N}\sum_{1,2,3,4}\delta_{1-2-3+4}(2\gamma_{3-4}a_1^\dagger a_2 b_3^\dagger b_4 + \gamma_4 a_1^\dagger a_2 a_3 a_4 \\ &+ \gamma_1 a_1^\dagger b_2^\dagger b_3^\dagger b_4) + \frac{2D}{N}\sum_{1,2,3,4}\delta_{1+2-3-4}(a_1^\dagger a_2^\dagger a_3 a_4 + b_1^\dagger b_2^\dagger b_3 b_4) \\ &- h_z\sum_{\mathbf{k}}(a_{\mathbf{k}}^\dagger a_{\mathbf{k}} - b_{\mathbf{k}}^\dagger b_{\mathbf{k}}),\end{aligned} \tag{42}$$

where for the square lattice

$$\gamma_{\mathbf{k}} = \frac{1}{z}\sum_{nn} e^{i\mathbf{k}\cdot\boldsymbol{\delta}} = \frac{1}{2}(\cos k_x + \cos k_y). \tag{43}$$

To diagonalize the quadratic part of the Hamiltonian, we use a standard Bogoliubov transformation

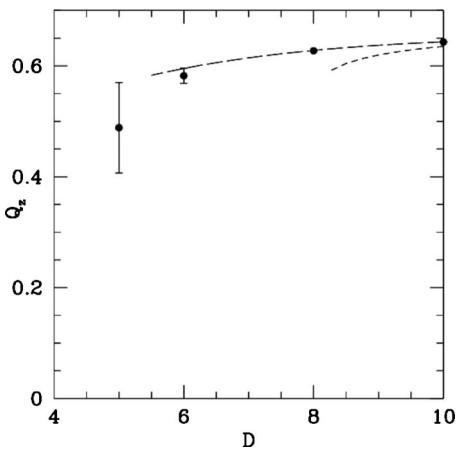

FIG. 10. Quadratic order parameter Q_z for the square lattice in the QPM phase as a function of D. Conventions as in Fig. 8.

$$a_{\mathbf{k}} = u_{\mathbf{k}} A_{\mathbf{k}} - v_{\mathbf{k}} B_{\mathbf{k}}^{\dagger},$$

$$b_{\mathbf{k}} = -v_{\mathbf{k}} A_{\mathbf{k}}^{\dagger} + u_{\mathbf{k}} B_{\mathbf{k}} \tag{44}$$

with $u_{\mathbf{k}} = \cosh \Theta_{\mathbf{k}}$ and $v_{\mathbf{k}} = \sinh \Theta_{\mathbf{k}}$.

This gives, after some algebra,

$$\mathcal{H} = N\mathcal{E}_0 + \sum_{\mathbf{k}} (\Omega_{\mathbf{k}}^A A_{\mathbf{k}}^{\dagger} A_{\mathbf{k}} + \Omega_{\mathbf{k}}^B B_{\mathbf{k}}^{\dagger} B_{\mathbf{k}}) + \sum_{\mathbf{k}} V_{\mathbf{k}} (A_{\mathbf{k}}^{\dagger} B_{\mathbf{k}}^{\dagger} + A_{\mathbf{k}} B_{\mathbf{k}}) + \text{quartic terms}, \tag{45}$$

where

$$\mathcal{E}_0 = -S^2 \left(\frac{zJ}{2} - D \right) + S(zJ - D) T_1 - zJST_4 - \frac{zJ}{2} (T_1 - T_4)^2 + 2DT_1^2, \tag{46}$$

$$\Omega_{\mathbf{k}}^{A,B} = [zJ(S - T_1 + T_4) - D(S - 4T_1)] \cosh 2\Theta_{\mathbf{k}} - zJ(S - T_1 + T_4) \gamma_{\mathbf{k}} \sinh 2\Theta_{\mathbf{k}} \mp h_z, \tag{47}$$

$$V_{\mathbf{k}} = zJ(S - T_1 + T_4) \gamma_{\mathbf{k}} \cosh 2\Theta_{\mathbf{k}} - [zJ(S - T_1 + T_4) - D(S - 4T_1)] \sinh 2\Theta_{\mathbf{k}}. \tag{48}$$

Diagonalization requires

$$\tanh 2\Theta_{\mathbf{k}} = \frac{Q\gamma_{\mathbf{k}}}{P}, \tag{49}$$

where

$$P = zJ(S - T_1 + T_4) - D(S - 4T_1),$$

$$Q = zJ(S - T_1 + T_4) \gamma_{\mathbf{k}}. \tag{50}$$

Then

$$\mathcal{H} = N\mathcal{E}_0 + \sum_{\mathbf{k}} (\omega_{\mathbf{k}}^A A_{\mathbf{k}}^{\dagger} A_{\mathbf{k}} + \omega_{\mathbf{k}}^B B_{\mathbf{k}}^{\dagger} B_{\mathbf{k}}) \tag{51}$$

with $\omega_{\mathbf{k}}^{A,B} = \omega_{\mathbf{k}} \mp h_z$,

$$\omega_{\mathbf{k}} = \sqrt{P^2 - (Q\gamma_{\mathbf{k}})^2}. \tag{52}$$

A. Phase boundaries

At leading order, we have that the ground-state energy in the Néel phase is

$$\mathcal{E}_0^{\text{Neel}} = -\frac{1}{2} S^2 (zJ - 2D) \tag{53}$$

while in the FM phase,

$$\mathcal{E}_0^{\text{FM}} = \frac{1}{2} S^2 (zJ + 2D - h_z). \tag{54}$$

These coincide at

$$h_{z,cA} = zJ, \tag{55}$$

which marks the first-order transition between the two phases at this order. At second order, the Néel results are modified and the transition point must be determined numerically. The results are shown in the phase diagram in Fig. 1 for the square lattice case, where it can be seen that the FM boundary lies slightly above the first-order estimate $h_{z,cA} = 4J$.

The minimum-energy gap at $\mathbf{k} = \mathbf{0}$ is

$$\epsilon_{\mathbf{k}}^{+} = S(\sqrt{D^2 - 2zJD}) \tag{56}$$

in leading order. This vanishes at $h_z = \sqrt{D^2 - 2zJD}$, which would mark the limit of the Néel phase at small D, except that the spin-flop ground-state energy falls below that of the Néel energy before that indicating a first-order transition. A numerical calculation of the boundary line $h_{z,cB}$ between the Néel and spin-flop phases is also shown in Fig. 1.

B. Order parameters

The staggered magnetization in the z direction

$$M_i^z = \frac{1}{N} \left\langle \sum_{i \in A} S_i^z - \sum_{j \in B} S_j^z \right\rangle_0$$

$$= S - \frac{1}{N} \sum_{\mathbf{k}} \langle a_{\mathbf{k}}^{\dagger} a_{\mathbf{k}} + b_{\mathbf{k}}^{\dagger} b_{\mathbf{k}} \rangle_0$$

$$= S - T_1 \tag{57}$$

up to second order in $1/S$. This remains independent of h_z up to the transition point.

V. SUMMARY AND CONCLUSIONS

We have explored some spin-wave approaches to the spin-1 model given in Eq. (1), using a different approach in each phase. In the Néel antiferromagnetic phase we use a standard Dyson-Maleev approach and the effect of the magnetic field is almost trivial, so we need not consider this phase further.

In the spin-flop phase we have used a Holstein-Primakoff transformation and a standard $1/S$ expansion approach, choosing our quantization axes in canted directions on the two sublattices as shown in Fig. 2, to match the expected classical configuration. We have shown analytically that the Goldstone theorem is respected in this formulation through second order in $1/S$, provided each quantity is strictly expanded in powers of $1/S$. The expansion converges well, and is accurate, for small D. It will also be accurate (at second order) near the ferromagnetic boundary $H_{z,cC}$, where the quantum fluctuations die away.

The results are not accurate, however, at large D near the QPM phase boundary. This is not surprising, perhaps, since the QPM phase does not exist in the classical (large S) limit. Inclusion of higher order terms might help to fix the problem, but they will be hard to calculate in a consistent fashion, so that we conclude that in this region the $1/S$ expansion is not very useful.

In the quantum paramagnetic phase we have used a different approach, where the vacuum state is taken as that with $S^z = 0$ at every site and a pair of Holstein-Primakoff boson

fields are introduced to describe the excitations to $S^z=\pm 1$ states. This approach gives good results at large positive D, but is again inaccurate at smaller D, near the QPM phase boundary.

It has been suggested[34] that these problems might be overcome in a "generalized" spin-wave approach in which a unitary transformation between the three $S=1$ basis states is made to establish an optimal vacuum state before the transformation to boson fields is performed. The Schwinger boson mean-field approach of Wang and Wang[31] is an approach of this sort and certainly it gives much better results in the region of the phase boundary.

The calculations in this paper have been carried out for the special case of uniform exchange, $\Delta=1$. This restriction could easily be lifted but to explore the possibility of biconical or supersolid phases using the $1/S$ expansion would require some rather complicated and delicate calculations. Again, a generalized spin-wave approach might be more useful. As a final technical note, we have chosen to use the Holstein-Primakoff formalism in this paper to maintain an explicitly Hermitian Hamiltonian but a Dyson-Maleev transformation might give simpler results and less singular behavior, as is often the case.

ACKNOWLEDGMENTS

We are grateful to Cristian Batista for introducing us to this problem and for very enlightening discussions. This research was undertaken on the NCI National Facility in Canberra, Australia, which is supported by the Australian Commonwealth Government. O.R. thanks CAPES for the financial support.

APPENDIX A

The bosonic equivalent of Hamiltonian (2) is

$$\begin{aligned}\mathcal{H}=&N\left[S^2\left(D\sin^2\theta-\frac{zJ}{2}\cos 2\theta-h_z\sin\theta\right)\right]+\frac{SD}{2}\cos^2\theta+\sum_i\eta_i(a_i+a_i^\dagger)\sqrt{\frac{S}{2}}\left\{S[(zJ+D)\sin 2\theta-h_z\cos\theta]-\frac{D}{2}\sin 2\theta\right\}\\&+\sum_i a_ia_i^\dagger\left\{S[zJ\cos 2\theta+h_z\sin\theta+D(-2+3\cos^2\theta)]+\frac{D}{2}(2-3\cos^2\theta)\right\}+\sum_i(a_i^2+a_i^{\dagger 2})(4S-1)\frac{D}{8}\cos^2\theta-\sum_{\langle i,j\rangle}(a_ia_j\\&+a_i^\dagger a_j^\dagger)SJ\cos^2\theta+\sum_{\langle i,j\rangle}(a_ia_j^\dagger+a_i^\dagger a_j)SJ\sin^2\theta+\sum_i\eta_i(a_i^{\dagger 2}a_i+a_i^\dagger a_i^2)\sqrt{\frac{S}{2}}\left[\frac{h_z}{4}\cos\theta-\frac{1}{4}(5D+zJ)\sin 2\theta\right]-\sum_i(a_i^{\dagger 3}a_i\\&+a_i^\dagger a_i^3)\frac{D}{4}\cos^2\theta+\sum_{\langle i,j\rangle}\eta_i[a_i^\dagger a_i(a_j+a_j^\dagger)]2J\sqrt{\frac{S}{2}}\sin 2\theta-\sum_i a_i^{\dagger 2}a_i^2\frac{D}{2}(3\cos^2\theta-2)-\sum_i(a_i^\dagger a_ia_j^\dagger a_j)J\cos 2\theta+\sum_{\langle i,j\rangle}(a_i^\dagger a_i^2a_j\\&+a_i^\dagger a_i^{\dagger 2}a_j+a_j^\dagger a_i^{\dagger 2}a_i+a_j^\dagger a_i^2a_i)\frac{J}{4}\cos^2\theta-\sum_{\langle i,j\rangle}(a_i^{\dagger 2}a_ia_j+a_i^\dagger a_j^\dagger a_j^2+a_j^\dagger a_i^\dagger a_i^2+a_j^{\dagger 2}a_ia_i)\frac{J}{4}\sin^2\theta+\text{terms of }\mathcal{O}(S^{-1/2}).\end{aligned}\tag{A1}$$

Next, we perform a Fourier transformation (5), to obtain a momentum space version of the Hamiltonian

$$\begin{aligned}\mathcal{H}=&N\left[S^2\left(D\sin^2\theta-\frac{zJ}{2}\cos 2\theta-h_z\sin\theta\right)\right]+\frac{SD}{2}\cos^2\theta+\sqrt{\frac{NS}{2}}(a_{\mathbf{Q}}+a_{\mathbf{Q}}^\dagger)\left\{S[(zJ+D)\sin 2\theta-h_z\cos\theta]-\frac{D}{2}\sin 2\theta\right\}\\&+\sum_{\mathbf{k}}a_{\mathbf{k}}^\dagger a_{\mathbf{k}}\left\{S[zJ\cos 2\theta+h_z\sin\theta+D(-2+3\cos^2\theta)]+\frac{D}{2}(2-3\cos^2\theta)\right\}+\sum_{\mathbf{k}}(a_{\mathbf{k}}a_{-\mathbf{k}}+a_{\mathbf{k}}^\dagger a_{-\mathbf{k}}^\dagger)\left[(4S-1)\frac{D}{8}\cos^2\theta\right.\\&\left.-\frac{zJ}{2}S\gamma_{\mathbf{k}}\cos^2\theta\right]+\sum_k(a_k^\dagger a_k)SzJ\gamma_{\mathbf{k}}\sin^2\theta+\frac{1}{\sqrt{N}}\sum_{1,2,3}(a_1^\dagger a_2^\dagger a_3+a_3^\dagger a_2a_1)\delta_{1+2-3-Q}\sqrt{\frac{S}{2}}\left[\frac{h_z}{4}\cos\theta-\frac{1}{4}(5D+zJ)\sin 2\theta\right]\\&+\frac{1}{\sqrt{N}}\sum_{1,2,3}(a_1^\dagger a_2a_3+\text{H.c.})zJ\gamma_3\delta_{1-2-3-Q}\sqrt{\frac{S}{2}}\sin 2\theta-\frac{1}{N}\sum_{1-4}a_1^\dagger a_2^\dagger a_3a_4\gamma_{2-4}\delta_{1+2-3-4}\frac{zJ}{2}\cos 2\theta\\&-\frac{1}{N}\sum_{1,2,3,4}a_1^\dagger a_2^\dagger a_3a_4\delta_{1+2-3-4}\frac{D}{2}(3\cos^2\theta-2)-\frac{1}{N}\sum_{1-4}(a_1^\dagger a_2^\dagger a_3^\dagger a_4+\text{H.c.})\delta_{1+2+3-4}\frac{D}{4}\cos^2\theta+\frac{1}{N}\sum_{1-4}(a_1^\dagger a_2a_3a_4\\&+\text{H.c.})\gamma_4\delta_{1-2-3-4}\frac{zJ}{4}\cos^2\theta-\frac{1}{N}\sum_{1-4}(a_1^\dagger a_2a_3a_4+\text{H.c.})\gamma_4\delta_{1+2-3-4}\frac{zJ}{4}\sin^2\theta+\text{terms of }\mathcal{O}(S^{-1/2}),\end{aligned}\tag{A2}$$

where z is the coordination number of the bipartite lattice, $\mathbf{Q}=(\pi,\pi)$ is the Néel momentum, and $\gamma_{\mathbf{k}}$ is the structure factor $\gamma_{\mathbf{k}}=\frac{1}{z}\Sigma_\delta e^{i\mathbf{k}\cdot\boldsymbol{\delta}}$ [for the square lattice $\gamma_{\mathbf{k}}=(\cos k_x+\cos k_y)/2$].

After the Bogoliubov transformation (6), the coefficient functions in Eq. (7) are

$$\mathcal{E}_0 = S^2\left(D\sin^2\theta - \frac{zJ}{2}\cos 2\theta - h_z\sin\theta\right) + S\left\{\frac{D}{2}\cos^2\theta + T_1[zJ\cos 2\theta + h_z\sin\theta + D(-2+3\cos^2\theta)] + T_2 D\cos^2\theta - T_4 zJ\cos^2\theta + T_3 zJ\sin^2\theta\right\} + T_1 D\left(1-\frac{3}{2}\cos^2\theta\right) - T_2\frac{D}{4}\cos^2\theta + (T_2^2+2T_1^2)D\left(1-\frac{3}{2}\cos^2\theta\right) - \frac{3}{2}T_1T_2D\cos^2\theta - (T_4^2+T_1^2+T_3^2)\frac{zJ}{2}\cos 2\theta + (2T_1T_4+T_2T_3)\frac{zJ}{2}\cos^2\theta - (T_2T_4+2T_1T_3)\frac{zJ}{2}\sin^2\theta, \tag{A3}$$

$$\mathcal{C} = \sqrt{\frac{S}{2}}\left\{S[(zJ+D)\sin 2\theta - h_z\cos\theta] - \frac{D}{2}\sin 2\theta\right\} + (T_2+2T_1)\left[\frac{h_z}{4}\cos\theta - \frac{1}{4}(5D+zJ)\sin 2\theta\right] + (-T_1+T_3+T_4)zJ\sin 2\theta, \tag{A4}$$

$$\mathcal{A}_{\mathbf{k}} = S\{[zJ\cos 2\theta + h_z\sin\theta + D(-2+3\cos^2\theta)] + zJ\gamma_{\mathbf{k}}\sin^2\theta\} + \frac{D}{2}(2-3\cos^2\theta) + 2T_1D(2-3\cos^2\theta) - \frac{3}{2}T_2D\cos^2\theta - (T_1+T_3\gamma_{\mathbf{k}})zJ\cos 2\theta + (2T_4+T_2\gamma_{\mathbf{k}})\frac{zJ}{2}\cos^2\theta - (T_3+T_1\gamma_{\mathbf{k}})zJ\sin 2\theta, \tag{A5}$$

$$\mathcal{B}_{\mathbf{k}} = (4S-1)\frac{D}{4}\cos^2\theta - \gamma_{\mathbf{k}}SzJ\cos^2\theta + T_2D(2-3\cos^2\theta) - \frac{3}{2}T_1D\cos^2\theta - T_4\gamma_{\mathbf{k}}zJ\cos 2\theta + (T_3+2T_1\gamma_{\mathbf{k}})\frac{zJ}{2}\cos^2\theta - (T_4+T_2\gamma_{\mathbf{k}})\frac{zJ}{2}\sin^2\theta, \tag{A6}$$

$$\mathcal{D}^{(1)} = \sqrt{\frac{S}{2}}\left[\frac{h_z}{4}\cos\theta - \frac{1}{4}(5D+zJ)\sin 2\theta\right], \tag{A7}$$

$$\mathcal{D}^{(2)} = zJ\sqrt{\frac{S}{2}}\sin 2\theta. \tag{A8}$$

Here T_1, T_2, T_3, and T_4 are contraction sums arising from the normal ordering process,

$$T_1 = \frac{1}{N}\sum_{\mathbf{k}} v_{\mathbf{k}}^2,$$

$$T_2 = \frac{1}{N}\sum_{\mathbf{k}} u_{\mathbf{k}}v_{\mathbf{k}},$$

$$T_3 = \frac{1}{N}\sum_{\mathbf{k}} v_{\mathbf{k}}^2\gamma_{\mathbf{k}},$$

$$T_4 = \frac{1}{N}\sum_{\mathbf{k}} u_{\mathbf{k}}v_{\mathbf{k}}\gamma_{\mathbf{k}}, \tag{A9}$$

and give corrections to the classical results due to quantum fluctuations.

APPENDIX B

Verification of Goldstone theorem

First, use Eq. (8) to eliminate the magnetic field h_z in favor of the angle θ, being careful to expand strictly to next-to-leading order in $1/S$,

$$h_z = 2\sin\theta(zJ+D)\left[1 - \frac{D}{S}\sin\theta(1+4T_1+2T_2) + \frac{2zJ}{S}\sin\theta(T_3+T_4-T_1)\right]. \tag{B1}$$

Then at $\gamma_{\mathbf{k}}\to -1$ we find

$$\mathcal{A}_{\mathbf{k}} = \left[S(zJ+D) - \frac{D}{2}\right]\cos^2\theta - T_1(2D+zJ)\cos^2\theta + T_2\left[\frac{\cos^2\theta}{2}(D-zJ) - 2D\right] + T_3zJ\cos^2\theta + T_4zJ(2-\cos^2\theta) \equiv \mathcal{A}_{\mathbf{k}}^0 + \delta\mathcal{A}_{\mathbf{k}}, \tag{B2}$$

where $\mathcal{A}_{\mathbf{k}}^0$ is the $\mathcal{O}(S)$ term, and $\delta\mathcal{A}_{\mathbf{k}}$ the term of $\mathcal{O}(1)$, and similarly

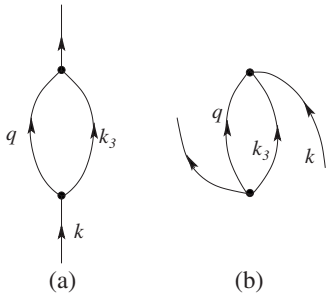

FIG. 11. The perturbation diagrams that contribute to the single-particle energy.

$$\mathcal{B}_{\mathbf{k}} = \left[S(zJ+D) - \frac{D}{4} \right] \cos^2\theta - T_1 \left(\frac{3}{2} D + zJ \right) \cos^2\theta + T_2 \left[D(2 - 3\cos^2\theta) + \frac{zJ}{2} \sin^2\theta \right] + T_3 \frac{zJ}{2} \cos^2\theta + T_4 zJ \left(1 - \frac{5}{2} \sin^2\theta \right) \equiv \mathcal{B}^0_{\mathbf{k}} + \delta\mathcal{B}_{\mathbf{k}}. \tag{B3}$$

Then to $\mathcal{O}(1)$

$$\omega_{\mathbf{k}} = \omega^0_{\mathbf{k}} + \delta\omega_{\mathbf{k}}, \tag{B4}$$

where $\omega^0_{\mathbf{k}} = \sqrt{(\mathcal{A}^0_{\mathbf{k}})^2 - (\mathcal{B}^0_{\mathbf{k}})^2}$ and

$$\delta\omega_{\mathbf{k}} = \frac{1}{2\omega^0_{\mathbf{k}}} (\mathcal{A}^0_{\mathbf{k}} \delta\mathcal{A}_{\mathbf{k}} - \mathcal{B}^0_{\mathbf{k}} \delta\mathcal{B}_{\mathbf{k}}),$$

$$= \frac{S(zJ+D)}{2\omega^0_{\mathbf{k}}} \left\{ D\cos^2\theta \left(-\frac{1}{4} - \frac{T_1}{2} + \frac{7}{2} T_2 \right) - 4DT_2 + zJ\cos^2\theta \left(\frac{T_3}{2} - \frac{7}{2} T_4 \right) + zJ \left(-\frac{T_2}{2} + \frac{7}{2} T_4 \right) \right\}. \tag{B5}$$

If we express $T_1, \ldots, T_4$ as integrals as in Eq. (10), then this expression reduces to

$$\delta\omega_{\mathbf{k}} = \frac{S^2(zJ+D)}{2\omega^0_{\mathbf{k}} N} \cos^2\theta \sin^2 2\theta \sum_{\mathbf{q}} \frac{(D - zJ\gamma_{\mathbf{q}})^2}{\omega^0_{\mathbf{q}}}. \tag{B6}$$

Now since $\omega^0_{\mathbf{k}} \to 0$ as $\mathbf{k} \to \mathbf{Q}$ the term $\delta\omega_{\mathbf{k}}$ actually diverges like $|\mathbf{k} - \mathbf{Q}|^{-1}$ in this limit. But there are further contributions to the single-particle energy at this order, coming from the perturbation diagrams, Figs. 11(a) and 11(b). Their contributions are given by

$$\Delta\epsilon^{(a)}_{\mathbf{k}} = \frac{S}{N} \sum_{\mathbf{q}} \left. \frac{|\Phi^{(2)}(\mathbf{q}, \mathbf{k}_3, \mathbf{k})|^2}{\omega^0_{\mathbf{k}} - \omega^0_{\mathbf{q}} - \omega^0_{\mathbf{k}_3}} \right|_{\mathbf{k}_3 = \mathbf{k} - \mathbf{q} + \mathbf{Q}}, \tag{B7}$$

$$\Delta\epsilon^{(b)}_{\mathbf{k}} = -9 \frac{S}{N} \sum_{\mathbf{q}} \left. \frac{|\Phi^{(1)}(\mathbf{q}, \mathbf{k}, \mathbf{k}_3)|^2}{\omega^0_{\mathbf{k}} + \omega^0_{\mathbf{q}} + \omega^0_{\mathbf{k}_3}} \right|_{\mathbf{k}_3 = -\mathbf{k} - \mathbf{q} + \mathbf{Q}}, \tag{B8}$$

where $\Phi^{(1)}$ and $\Phi^{(2)}$ are given by Eqs. (13) and (14), respectively. Now these terms also diverge as $\mathbf{k} \to \mathbf{Q}$, because in that limit $u_{\mathbf{k}} \sim -v_{\mathbf{k}} \sim |\mathbf{k} - \mathbf{Q}|^{-1}$. Explicit calculation shows that through terms $\mathcal{O}(1)$ in an expansion of powers of $|\mathbf{k}'| = |\mathbf{k} - \mathbf{Q}|$,

$$\Delta\epsilon^{(a)}_{\mathbf{k}} + \Delta\epsilon^{(b)}_{\mathbf{k}} = -\frac{S^2(zJ+D)}{2\omega^0_{\mathbf{k}} N} \cos^2\theta \sin^2 2\theta \times \sum_{\mathbf{q}} \frac{(D - zJ\gamma_{\mathbf{q}})^2}{\omega^0_{\mathbf{q}}}, \tag{B9}$$

exactly canceling the term $\delta\omega_{\mathbf{k}}$ of Eq. (B6). Hence the total excitation energy

$$\epsilon_{\mathbf{k}} = \omega_{\mathbf{k}} + \Delta\epsilon^{(a)}_{\mathbf{k}} + \Delta\epsilon^{(b)}_{\mathbf{k}} \tag{B10}$$

vanishes as $\mathbf{k} \to \mathbf{Q}$, to this order is $1/S$, in accordance with the Goldstone theorem.

[1] E. Kim and M. H. W. Chan, Nature (London) **427**, 225 (2004); Science **305**, 1941 (2004).
[2] K.-K. Ng and T. K. Lee, Phys. Rev. Lett. **97**, 127204 (2006).
[3] P. Sengupta and C. D. Batista, Phys. Rev. Lett. **98**, 227201 (2007).
[4] P. Sengupta and C. D. Batista, J. Appl. Phys. **103**, 07C709 (2008).
[5] T. Matsubara and H. Matsuda, Prog. Theor. Phys. **16**, 569 (1956).
[6] D. P. Landau and K. Binder, Phys. Rev. B **24**, 1391 (1981).
[7] M. Steiner, K. Kakurai, J. K. Kiems, and D. Petitgrand, J. Appl. Phys. **61**, 3953 (1987).
[8] J. P. Renard, M. Verdaguer, L. P. Regnault, W. A. C. Erkelens, and J. Rossat-Mignod, J. Appl. Phys. **63**, 3538 (1988).
[9] M. Orendac, A. Orendacova, J. Cernak, A. Feher, P. J. C. Signore, M. W. Meisel, S. Merah, and M. Verdaguer, Phys. Rev. B **52**, 3435 (1995).
[10] S. A. Zvyagin, J. Wosnitza, C. D. Batista, M. Tsukamoto, N. Kawashima, J. Krzystek, V. S. Zapf, M. Jaime, N. F. Oliviera, Jr., and A. Paduan-Filho, Phys. Rev. Lett. **98**, 047205 (2007).
[11] S. A. Zvyagin, C. D. Batista, J. Krzystek, V. S. Zapf, M. Jaime, A. Paduan-Filho, and J. Wosnitza, Physica B **403**, 1497 (2008).
[12] A. W. Sandvik, Phys. Rev. B **59**, R14157 (1999).
[13] M. Holtschneider, W. Selke, and R. Leidl, Phys. Rev. B **72**, 064443 (2005).
[14] M. Holtschneider and W. Selke, Phys. Rev. B **76**, 220405(R) (2007).
[15] M. Holtschneider and W. Selke, Eur. Phys. J. B **62**, 147 (2008), and references therein.
[16] D. Peters, I. P. McCulloch, and W. Selke, Phys. Rev. B **79**,

132406 (2009).
[17] T. Roscilde and S. Haas, Phys. Rev. Lett. **99**, 047205 (2007).
[18] K. Osano, H. Shiba, and Y. Endoh, Prog. Theor. Phys. **67**, 995 (1982).
[19] S. Gluzman, Z. Phys. B: Condens. Matter **90**, 313 (1993).
[20] M. E. Zhitomirsky and T. Nikuni, Phys. Rev. B **57**, 5013 (1998).
[21] M. E. Zhitomirsky and T. Nikuni, Physica B **241-243**, 573 (1998).
[22] M. E. Zhitomirsky and A. L. Chernyshev, Phys. Rev. Lett. **82**, 4536 (1999).
[23] A. L. Chernyshev and M. E. Zhitomirsky, Phys. Rev. B **79**, 174402 (2009).
[24] N. Papanicolaou, Z. Phys. B: Condens. Matter **61**, 159 (1985).
[25] N. Papanicolaou and P. Spathis, J. Phys.: Condens. Matter **2**, 6575 (1990).
[26] J. Oitmaa and C. J. Hamer, Phys. Rev. B **77**, 224435 (2008).
[27] M. S. Yang and K. H. Mütter, Z. Phys. B: Condens. Matter **104**, 117 (1997).
[28] Zheng Weihong, J. Oitmaa, and C. J. Hamer, Phys. Rev. B **43**, 8321 (1991).
[29] W. H. Wong, C. F. Lo, and Y. L. Wang, Phys. Rev. B **50**, 6126 (1994).
[30] H. Q. Lin and V. J. Emery, Phys. Rev. B **40**, 2730 (1989).
[31] H.-T. Wang and Y. Wang, Phys. Rev. B **71**, 104429 (2005).
[32] J. Holstein and N. Primakoff, Phys. Rev. **58**, 1098 (1940).
[33] B. I. Halperin and P. C. Hohenberg, Phys. Rev. **188**, 898 (1969).
[34] C. D. Batista (private communication).